Analytical model of the crossed wire particle velocity sensor

Twan Spil s1227718
Bachelor assignment committee
prof.dr.ir. GJM Krijnen
prof.dr.ir. A. de Boer
ir. O. Pjetri

July 4, 2014

Abstract

The subject of this Bachelor Assignment is acoustic particle velocity sensing based on thermal sensors. An acoustic particle velocity sensor is a sensor which is able to measure sound waves not through variations in pressure but through particle velocity. The particle velocity is measured by variations in resistance due to flow induced changes in temperature. In this report an analytical model for the temperature distribution is developed. From this the temperature perturbation under influence of a flow is calculated, a comparison with measurements shows that the temperature perturbation model still needs refinement.

Contents

Chapter 1

Introduction

The subject of this Bachelor Assignment is acoustic particle velocity sensing based on thermal sensors. There are various configurations for these sensors, most of them relying on either two heated wires, or one heated wire and two measurement wires [3, 4]. These sensors work as follows, a current is put through the heating wire(s) and power is dissipated as heat. The heat will cause a thermal profile over the sensor. When an acoustic particle velocity, aka a sound wave, travels over the sensor, the thermal profile will be disturbed. This flow disturbance leads to a temperature difference between the measuring wires that causes a change in resistance which is then measured by measuring the voltage over the wires when an equal current flows through the wires. For the configurations with either two heated wires, or one heated wire and two measurement wires an analytical model has already been developed.

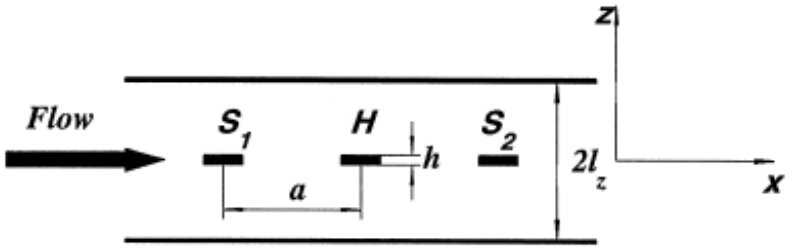

Figure 1.1: The configuration with one heater wire and two sensor wires for which an analytical model already has been developed [3]

In this work the focus is on a so called crossed wire sensor geometry. The crossed wire sensor [2] deviates from previous configurations, because now the wires are both heaters and sense the resistance variations and more importantly, the temperature variations are caused by flows parallel to the wires and measured along the longitudinal direction, this is also illustrated in figure 1.2 (c). In the crossed wire sensor, the wires are heated by forcing a current through the wires this is illustrated in figure 1.2 (b). In a static situation when there is no particle velocity over the sensor, the thermal profile will be symmetric and the resistances of the wires will be equal. Due to an equal current being forced over the wires, the voltages will also be equal and the difference of the voltages between the ends of the wire will be zero. When a sound wave travels over the sensor, for example over R2 and R5, the resistance changes differently for R2 then it does for R5, and the difference between the voltage $V_{1+} - V_{1-}$ will be non-zero.
In this bachelor thesis I made an analytical model to gather more insight in how the various parameters affect the sensitivity of the sensor. The analytical model was made in a number of phases. I began with a single wire thermal profile, elaborated this to the crossed wires. Then I made a model

for the thermal profile when there is a static flow disturbance and finally I made a model for the thermal profile with dynamic flow disturbances. From these flow disturbances it is possible to predict the sensitivity. The model is compared with measurements to assess their predictive quality.

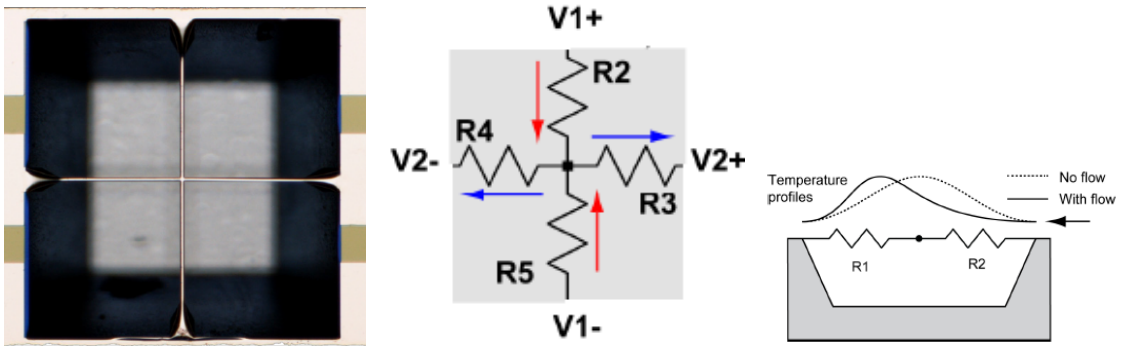

(a) (b) (c)

Figure 1.2: (a) Image from a top view of the crossed wire 2D particle velocity sensor [2] (b) A schematic of how the forced currents flow through the wires of the sensor (c) A drawing of how the flow affects the temperature profile over the wires (resistors)

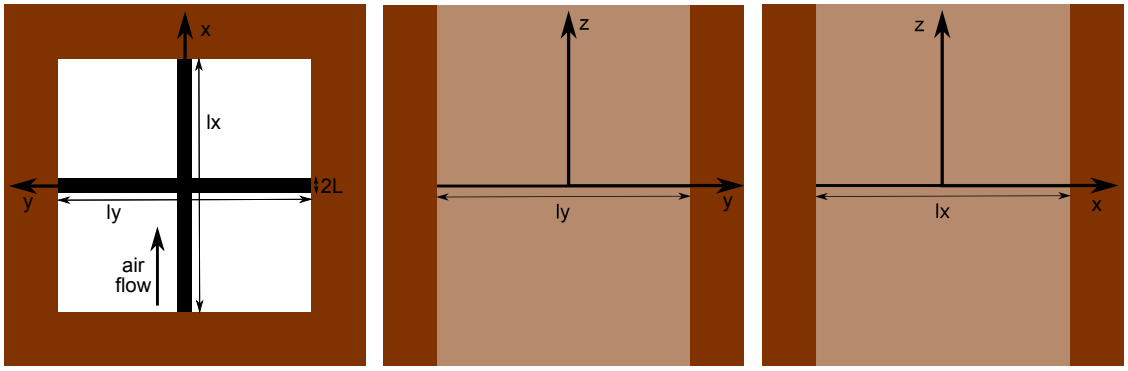

Figure 1.3: Geometry of the sensor used in analysis, the parts depicted in brown have an ambient temperature. Take note that in this geometry there are no walls in the z-direction, which is a simplification of the sensor which has a bottom located at 250 µm and that the walls that are depicted extend 'infinitely'

Chapter 2

Analytical model

2.1 Static thermal profile

2.1.1 One wire

To gather some insight I will start with a somewhat different geometry, which can be seen in figure 2.1. To make a analytical model for the thermal profile we start with the heat equation.

$$-\nabla(k\nabla T) = Q \tag{2.1}$$

Where k is the gas thermal conductivity, which has a dependence on T but for the sake of simplicity we assume it to be negligible. Q is the heat quantity produced by the wire. It is only non zero on the position where the wire is located and is distributed evenly along the wire that it can be written as.

$$Q = \frac{P}{l_y}\delta(x)\delta(z) \tag{2.2}$$

Where P is the power dissipated by the wires as heat and l_y the length of the wire. The positional dependence is taken into account with the delta functions, this can be done because the length of the wire is much bigger then the width or the thickness. Later on in this report the finite thickness is also taken into consideration. Putting the expression for Q into (2.1) together with the assumption that k does not depend on temperature nor position, results in a linear partial differential equation.

$$-k\left(\frac{\partial^2}{\partial x^2}+\frac{\partial^2}{\partial y^2}+\frac{\partial^2}{\partial z^2}\right)T(x,y,z) = Q \tag{2.3}$$

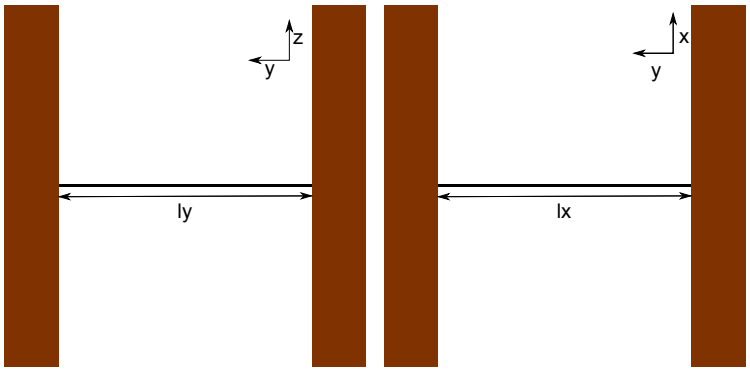

Figure 2.1: The geometry as used in this section, with the parts depicted in brown having an ambient temperature

We can solve this equation using eigenfunction expansion [1], we start with the homogeneous partial differential equation and solve for y with separation of variables. For the boundary condition we use that $T(x, \pm\frac{l_y}{2}, z) = 0$, where the ambient temperature is taken zero. The walls on $\pm\frac{l_y}{2}$ in figure 2.1 extent to infinity.

$$-k\left(\frac{\partial^2}{\partial x^2}+\frac{\partial^2}{\partial y^2}+\frac{\partial^2}{\partial z^2}\right)T(x,y,z)=0 \tag{2.4}$$

$$T(x,y,z) = Tx(x,z)Y(y) \tag{2.5}$$

$$-\frac{\left(\frac{\partial^2}{\partial x^2}+\frac{\partial^2}{\partial z^2}\right)Tx}{Tx} = \frac{\frac{\partial^2}{\partial y^2}Y}{Y} \tag{2.6}$$

$$\frac{\frac{\partial^2}{\partial y^2}Y}{Y} = -\lambda \tag{2.7}$$

$$\frac{\partial^2}{\partial y^2}Y + \lambda Y = 0 \tag{2.8}$$

$$Y(\pm\frac{l_y}{2}) = 0 \tag{2.9}$$

$$Y(y) = \cos\left(\frac{2\lambda_n y}{ly}\right) \tag{2.10}$$

$$\lambda_n = \frac{\pi}{2}(2n+1) \tag{2.11}$$

$$T(x,y,z) = \sum_{n=0}^{\infty} T_n(x,z)\cos\left(\frac{2\lambda_n y}{l_y}\right) \tag{2.12}$$

Filling this into (2.3) results in

$$\sum_{n=0}^{\infty}\left[\left(\frac{\partial^2}{\partial x^2}+\frac{\partial^2}{\partial z^2}\right)T_n-\left(\frac{2\lambda_n}{l_y}\right)^2 T_n\right]\cos\left(\frac{2\lambda_n y}{l_y}\right) = -\frac{P}{l_y k}\delta(x)\delta(z) \tag{2.13}$$

Due to orthogonality

$$\left(\frac{\partial^2}{\partial x^2}+\frac{\partial^2}{\partial z^2}\right)T_n-\left(\frac{2\lambda_n}{l_y}\right)^2 T_n = \frac{2}{l_y}\int_{-\frac{l_y}{2}}^{\frac{l_y}{2}} -\frac{P}{l_y k}\delta(x)\delta(z)\cos\left(\frac{2\lambda_n y}{l_y}\right)\mathrm{d}y \tag{2.14}$$

$$= -\frac{P}{l_y k}\delta(x)\delta(z)\frac{2\sin(\lambda_n)}{\lambda_n} \tag{2.15}$$

$$= -\frac{2(-1)^n}{\lambda_n}\frac{P}{l_y k}\delta(x)\delta(z) \tag{2.16}$$

Using the Fourier transform

$$\hat{T}_n(k_x,k_z) = \int_{-\infty}^{\infty}\int_{-\infty}^{\infty} T_n(x,z)e^{-i(k_x x+k_z z)}\mathrm{d}x\mathrm{d}z \tag{2.17}$$

to (2.16)

$$\left(-k_x^2+-k_z^2\right)\hat{T}_n-\left(\frac{2\lambda_n}{l_y}\right)\hat{T}_n = -\frac{2(-1)^n}{\lambda_n}\frac{P}{l_y k} \tag{2.18}$$

$$\hat{T}_n = \frac{\frac{2(-1)^n}{\lambda_n}\frac{P}{l_y}}{k_x^2+k_y^2+\left(\frac{2\lambda_n}{l_y}\right)^2} \tag{2.19}$$

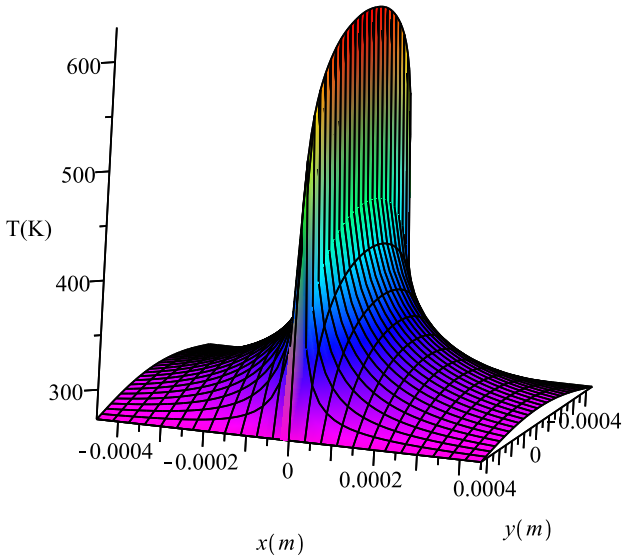

Figure 2.2: 3D plot of the temperature profile (2.22) depending on x and y with $z = 1\mu m$

The Fourier transform of a second kind modified Bessel function is

$$\mathscr{F}[K_0(ar)] = \frac{1}{2\pi}\frac{1}{k^2+a^2} \tag{2.20}$$

If we assume for our solution that the frequency is radial $k = \sqrt{k_x^2 + k_z^2}$ then we can take the inverse transform to get

$$T_n(x,z) = \frac{2(-1)^n}{\lambda_n}\frac{P}{2\pi l_y k}K_0\left(\frac{2\lambda_n\sqrt{x^2+z^2}}{l_y}\right) \tag{2.21}$$

Filling everything back together results in

$$T(x,y,z) = \sum_{n=0}^{\infty}\frac{2(-1)^n}{\lambda_n}\frac{P}{2\pi l_y k}K_0\left(\frac{2\lambda_n\sqrt{x^2+z^2}}{l_y}\right)\cos\left(\frac{2\lambda_n y}{l_y}\right) \tag{2.22}$$

A plot of this solution can be seen in figure 2.2. The parameters used for all the graphs in this chapter can be found in the table below.

l_y	l_x	$2L$	k	P	v
900 µm	900 µm	2 µm	0.0386 W K^{-1} m	26 mW	4.4×10^{-3} m s^{-1}

2.1.2 Two wires

Due to linearity of the heat equation it is possible to just add up the two thermal profiles for the two wires which are the same but with reversed x and y. Resulting in

$$T(x,y,z) = \sum_{n=0}^{\infty} \left[\frac{2(-1)^n}{\lambda_n} \frac{P}{2\pi l_y k} K_0\left(\frac{2\lambda_n \sqrt{x^2+z^2}}{l_y}\right) \cos\left(\frac{2\lambda_n y}{l_y}\right) + \frac{2(-1)^n}{\lambda_n} \frac{P}{2\pi l_x k} K_0\left(\frac{2\lambda_n \sqrt{y^2+z^2}}{l_x}\right) \cos\left(\frac{2\lambda_n x}{l_x}\right) \right] \tag{2.23}$$

This equation is plotted in figure 2.3

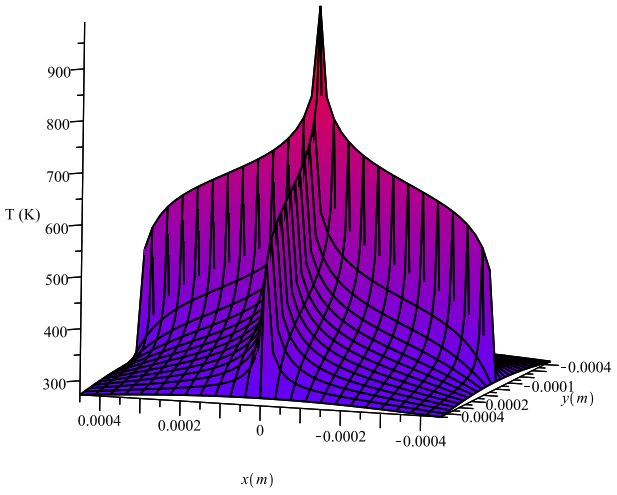

Figure 2.3: 3D plot of the temperature against x and y of the equation with two wires (2.23) with $z = 1\mu m$

2.2 Thermal heat profile with Finite width

2.2.1 One wire

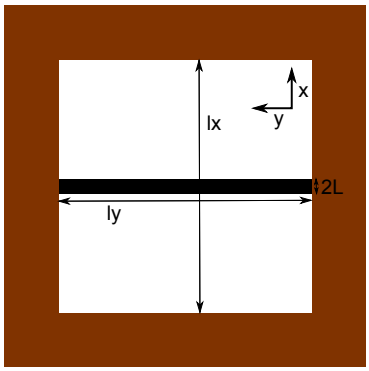

Figure 2.4: Geometry used for developing the analytical model for the thermal profile with a finite width

Starting from the same heat equation

$$-\nabla(k\nabla T) = Q \tag{2.24}$$

But now we take into account a finite width for the wires. The total width is $2L$

$$Q = \frac{P}{2Ll_y}F(x)\delta(z) \tag{2.25}$$

$$F(x) = \begin{Bmatrix} 1 & |x| < L \\ 0 & \text{otherwise} \end{Bmatrix} \tag{2.26}$$

Assuming that k is constant

$$\left(\frac{\partial^2}{\partial x^2} + \frac{\partial^2}{\partial y^2} + \frac{\partial^2}{\partial z^2}\right) T = -\frac{P}{2Lkl_y}F(x)\delta(z) \tag{2.27}$$

The boundary conditions

$$T(\pm\frac{l_x}{2}, y, z) = 0 \tag{2.28}$$

$$T(x, \pm\frac{l_y}{2}, z) = 0 \tag{2.29}$$

$$T(x, y, \pm\infty) = 0 \tag{2.30}$$

Using the method of eigenfunction expansion, first taking the homogeneous function, thus Q = 0 and

using the method of separation of variables.

$$\left(\frac{\partial^2}{\partial x^2}+\frac{\partial^2}{\partial y^2}+\frac{\partial^2}{\partial z^2}\right)T=0 \tag{2.31}$$

$$T(x,y,z)=\Theta(x,y)Z(z) \tag{2.32}$$

$$\frac{\left(\frac{\partial^2}{\partial x^2}+\frac{\partial^2}{\partial y^2}\right)\Theta(x,y)}{\Theta(x,y)}=\frac{\frac{\partial^2}{\partial z^2}Z(z)}{Z(z)} \tag{2.33}$$

$$\frac{\left(\frac{\partial^2}{\partial x^2}+\frac{\partial^2}{\partial y^2}\right)\Theta(x,y)}{\Theta(x,y)}=-\lambda \tag{2.34}$$

$$\Theta(x,y)=\cos\left(\frac{2\lambda_m y}{l_\mathrm{y}}\right)\cos\left(\frac{2\lambda_n x}{l_\mathrm{x}}\right) \tag{2.35}$$

With $\lambda_n=\frac{pi}{2}(2n+1)$ and $\lambda_m=\frac{pi}{2}(2m+1)$ such that the temperature is zero at the boundaries $\pm\frac{l_\mathrm{y}}{2}$ and $\pm\frac{l_\mathrm{x}}{2}$.

$$T(x,y,z)=\sum_{n=0}^{\infty}\sum_{m=0}^{\infty}T_{nm}(z)\cos\left(\frac{2\lambda_m y}{l_\mathrm{y}}\right)\cos\left(\frac{2\lambda_n x}{l_\mathrm{x}}\right) \tag{2.36}$$

Now filling this back into the heat equation we get

$$\sum_{n=0}^{\infty}\sum_{m=0}^{\infty}\left[\frac{\partial^2}{\partial z^2}T_{nm}-\left(\left(\frac{2\lambda_n}{l_\mathrm{x}}\right)^2+\left(\frac{2\lambda_m}{l_\mathrm{y}}\right)^2\right)T_{nm}\right]\cos\left(\frac{2\lambda_m y}{l_\mathrm{y}}\right)\cos\left(\frac{2\lambda_n x}{l_\mathrm{x}}\right) \tag{2.37}$$

$$=-\frac{P}{2Lkl_\mathrm{y}}F(x)\delta(z)$$

Due to orthogonality

$$\left(\frac{\partial^2}{\partial z^2}-\left(\frac{2\lambda_n}{l_\mathrm{x}}\right)^2-\left(\frac{2\lambda_m}{l_\mathrm{y}}\right)^2\right)T_{nm} \tag{2.38}$$

$$=-\frac{2}{l_\mathrm{y}}\frac{2}{l_\mathrm{x}}\int_{-\frac{l_\mathrm{x}}{2}}^{\frac{l_\mathrm{x}}{2}}\int_{-\frac{l_\mathrm{y}}{2}}^{\frac{l_\mathrm{y}}{2}}-\frac{P}{2Ll_\mathrm{y}k}F(x)\delta(z)\cos\left(\frac{2\lambda_m y}{l_\mathrm{y}}\right)\cos\left(\frac{2\lambda_n x}{l_\mathrm{x}}\right)\mathrm{d}y\mathrm{d}x \tag{2.39}$$

$$=-\frac{(-1)^m P}{\lambda_m Ll_\mathrm{y}k}\delta(z)\int_{-L}^{L}\cos\left(\frac{2\lambda_n x}{l_\mathrm{x}}\right)\mathrm{d}x \tag{2.40}$$

$$=-\frac{2(-1)^m}{\lambda_m\lambda_n}\frac{P}{Ll_\mathrm{y}k}\sin\left(\frac{2\lambda_n L}{l_\mathrm{x}}\right)\delta(z) \tag{2.41}$$

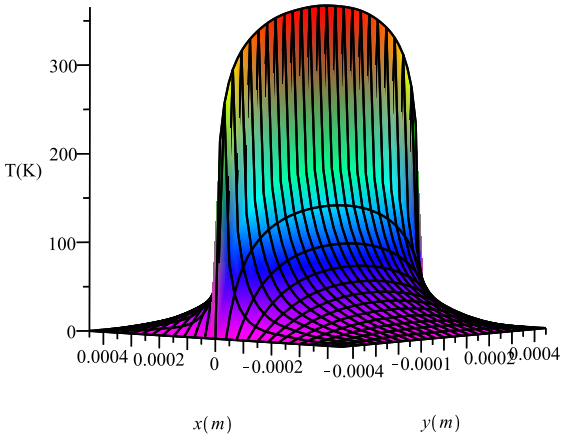

Figure 2.5: 3D plot of the temperature profile (2.47) depending on x and y with $z = 0$

Using the Fourier Transform

$$\hat{T}_{nm}(k_z) = \int_{-\infty}^{\infty} T_{nm} e^{-ik_z z} \mathrm{d}z \tag{2.42}$$

$$\left(k_z^2 + \left(\frac{2\lambda_n}{l_x}\right)^2 + \left(\frac{2\lambda_m}{l_y}\right)^2\right) \hat{T}_{nm} = \frac{2(-1)^m}{\lambda_m \lambda_n} \frac{P}{L l_y k} \sin\left(\frac{2\lambda_n L}{l_x}\right) \tag{2.43}$$

$$\hat{T}_{nm} = \frac{\frac{2(-1)^m}{\lambda_m \lambda_n} \frac{P}{L l_y k} \sin\left(\frac{2\lambda_n L}{l_x}\right)}{k_z^2 + \sqrt{\left(\frac{2\lambda_n}{l_x}\right)^2 + \left(\frac{2\lambda_m}{l_y}\right)^2}^2} \tag{2.44}$$

$$\mathscr{F}^{-1}\left(\frac{2a}{k_z^2 + a^2}\right) = \frac{e^{-a|x|}}{2\pi} \tag{2.45}$$

$$T_{nm} = \frac{\frac{(-1)^m}{\lambda_m \lambda_n} \frac{P}{L l_y k} \sin\left(\frac{2\lambda_n L}{l_x}\right)}{\sqrt{\left(\frac{2\lambda_n}{l_x}\right)^2 + \left(\frac{2\lambda_m}{l_y}\right)^2}} \exp\left(-\sqrt{\left(\frac{2\lambda_n}{l_x}\right)^2 + \left(\frac{2\lambda_m}{l_y}\right)^2} |z|\right) \tag{2.46}$$

Putting it all together, resulting in the solution

$$T(x,y,z) = \sum_{n=0}^{\infty} \sum_{m=0}^{\infty} \frac{(-1)^m}{\lambda_m \lambda_n \sigma_{nm}} \frac{P}{L l_y k} \sin\left(\frac{2\lambda_n L}{l_x}\right) \exp(-\sigma_{nm}|z|) \cos\left(\frac{2\lambda_m y}{l_y}\right) \cos\left(\frac{2\lambda_n x}{l_x}\right) \tag{2.47}$$

$$\sigma_{nm} = \sqrt{\left(\frac{2\lambda_n}{l_x}\right)^2 + \left(\frac{2\lambda_m}{l_y}\right)^2} \tag{2.48}$$

A plot of this can be seen in Figure 2.5.

2.2.2 Heat loss through the wire

Now that there is an expression for the thermal profile, it is possible to calculate if the assumption that the heat loss through the wire ends is small in comparison to the heat loss through the rest of the

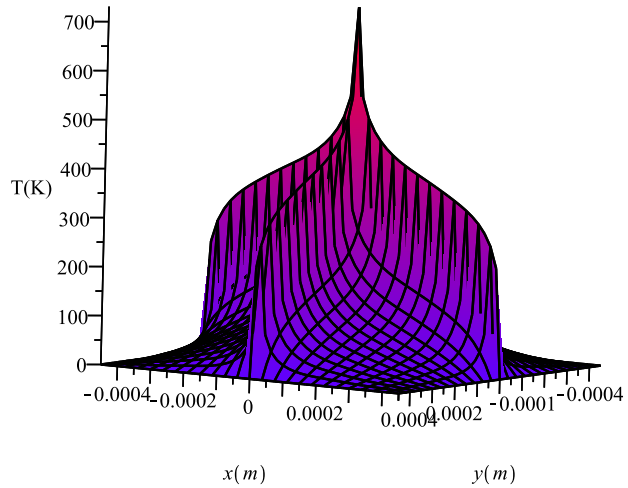

Figure 2.6: 3D plot of the temperature profile with two wires (2.50) depending on x and y with $z = 0$

walls. The heat power dissipated trough the beam ends ΔP, is the product of the heat flux through the wire ends and the area of the wire cross section.

$$\Delta P = 2k_{\mathrm{w}} \frac{\partial T}{\partial y}_{y=\frac{l_{\mathrm{y}}}{2}} h2L \tag{2.49}$$

Working this out and filling it in with $k_{\mathrm{w}} = 18.5\,\mathrm{W\,K^{-1}\,m}$ and $h = 0.1\,\mu\mathrm{m}$ results in $\frac{\Delta P}{P} = 0.0263$. So less then 3% of power is dissipated on the wire end, this means that the assumption that only a small portion of the power is dissipated at the wire ends.

2.2.3 Two wires

Using the thermal profile we got and combining it results in the following equation.

$$\begin{aligned} T(x,y,z) = &\sum_{n,m=0}^{\infty} \frac{(-1)^m}{\lambda_m \lambda_n \sigma_{nm}} \frac{P}{L l_{\mathrm{y}} k} \sin\left(\frac{2\lambda_n L}{l_{\mathrm{x}}}\right) \exp\left(-\sigma_{nm}|z|\right) \cos\left(\frac{2\lambda_m y}{l_{\mathrm{y}}}\right) \cos\left(\frac{2\lambda_n x}{l_{\mathrm{x}}}\right) \\ &+ \sum_{n,m=0}^{\infty} \frac{(-1)^m}{\lambda_m \lambda_n \sigma_{nm}} \frac{P}{L l_{\mathrm{x}} k} \sin\left(\frac{2\lambda_n L}{l_{\mathrm{y}}}\right) \exp\left(-\sigma_{nm}|z|\right) \cos\left(\frac{2\lambda_m x}{l_{\mathrm{x}}}\right) \cos\left(\frac{2\lambda_n y}{l_{\mathrm{y}}}\right) \end{aligned} \tag{2.50}$$

The plot can be seen in Figure 2.6.

2.2.4 Comparison with simulation

In figure 2.7 you can see a comparison between the thermal profile as calculated from the analytical model (2.50) and a simulation with the geometry of the actual sensor. The two profiles are almost the same, the middle point is higher in the model, because we put two thermal profiles over each other which causes the power where the two wires cross to be doubled. Also the temperature of the model overall is slightly higher then in the model, this can be due to not taking into account the bottom of the chip.

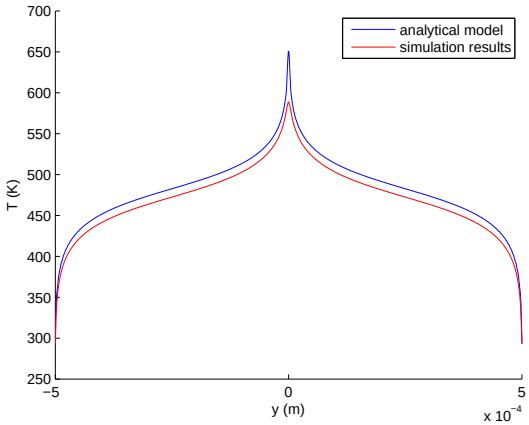

Figure 2.7: A plot of the temperature profile of the analytical model and temperature profile from the simulation against y with $x, z = 0$

2.3 Static disturbance thermal profile

2.3.1 Wire perpendicular to air flow

Due to the air flow there are two more terms in the heat equation.

$$\rho c_p \left(\frac{\partial}{\partial t} T + \mathbf{v} \cdot \nabla T \right) - \nabla (k \nabla T) = Q \tag{2.51}$$

Where v is the gas velocity, ρ and c_p the density and heat capacity of the gas, the heat capacity and density of the wires aren't taken into account in this equation, this is done for the sake of simplicity. The time differential of T is zero because T is assumed to have only a static disturbance, thus no dependence on time.
The convective term in equation (2.51) can be treated as a perturbation because the diffusion velocity is large in comparison with the forced convection caused by the particle velocity. Let's look at how long it takes for a particle to travel over the length of the sensor l_x: due to diffusion this time will be l_x^2/D with $D = k/\rho c_p \approx 1.9 \times 10^{-5}\,\mathrm{m^2\,s^{-1}}$, due to forced convection this time will be l_x/v. If we compare these times with each other

$$\frac{v}{D/l_\mathrm{x}} \ll 1 \tag{2.52}$$

Because the diffusion velocity $D/l_\mathrm{x} \approx 0.02\,\mathrm{m\,s^{-1}}$ is large in comparison with $v = 4.4 \times 10^{-3}\,\mathrm{m\,s^{-1}}$ (which corresponds to a very high acoustic pressure of 100 dB). Therefore we can consider the temperature as $T + \delta T$ where T is the temperature in non-flowing air that was already found and δT the perturbation caused by the flowing air. We will solve the case for air flowing in one direction $\mathbf{v} = (v_x, 0, 0)$.

$$\nabla^2 \delta T = \frac{v_x}{D} \frac{\partial}{\partial x} T \tag{2.53}$$

$$\frac{\partial}{\partial x} T = \sum_{n=0}^{\infty} \sum_{m=0}^{\infty} -C_{nm} \times \exp\left(-\sigma_{nm}|z|\right) \cos\left(\frac{2\lambda_m y}{l_\mathrm{y}}\right) \sin\left(\frac{2\lambda_n x}{l_\mathrm{x}}\right) \tag{2.54}$$

$$C_{nm} = \frac{2(-1)^m}{\lambda_m \sigma_{nm}} \frac{P}{L l_\mathrm{y} l_\mathrm{x} k} \sin\left(\frac{2\lambda_n L}{l_\mathrm{x}}\right) \tag{2.55}$$

$$\nabla^2 \delta T = \sum_{n=0}^{\infty} \sum_{m=0}^{\infty} -C_{nm} \frac{v_x}{D} \exp(-\sigma_{nm}|z|) \cos\left(\frac{2\lambda_m y}{l_\mathrm{y}}\right) \sin\left(\frac{2\lambda_n x}{l_\mathrm{x}}\right) \tag{2.56}$$

To solve this equation one should again use the eigenfunction expansion, but this time a cosine for the x-direction will not work, because the integral of a sine and cosine over the length of the wire results in zero. Thus we use a sine that satisfies the boundary conditions.

$$\delta T = \sum_{i=0}^{\infty}\sum_{j=1}^{\infty} \delta T_{ij}(z)\cos\left(\frac{2\lambda_i}{l_\mathrm{y}}y\right)\sin\left(\frac{2\pi j}{l_\mathrm{x}}x\right) \tag{2.57}$$

Substituting this into (2.56) and again orthogonalising the various terms yields

$$\begin{aligned}&\left(\frac{\partial^2}{\partial z^2} - \left(\frac{2\lambda_i}{l_\mathrm{y}}\right)^2 - \left(\frac{2\pi j}{l_\mathrm{x}}\right)^2\right)\delta T_{ij}(z) = \\ &\sum_{n,m=0}^{\infty}\Bigg[-C_{nm}\frac{v_x}{D}\exp(-\sigma_{nm}|z|)\times \\ &\frac{2}{l_\mathrm{y}}\int_{-\frac{l_\mathrm{y}}{2}}^{\frac{l_\mathrm{y}}{2}}\cos\left(\frac{2\lambda_m y}{l_\mathrm{y}}\right)\cos\left(\frac{2\lambda_i y}{l_\mathrm{y}}\right)\mathrm{d}y\frac{2}{l_\mathrm{x}}\int_{-\frac{l_\mathrm{x}}{2}}^{\frac{l_\mathrm{x}}{2}}\sin\left(\frac{2\lambda_n x}{l_\mathrm{x}}\right)\sin\left(\frac{2\pi j x}{l_\mathrm{x}}\right)\mathrm{d}x\Bigg]\end{aligned} \tag{2.58}$$

$$\frac{2}{l_\mathrm{y}}\int_{-\frac{l_\mathrm{y}}{2}}^{\frac{l_\mathrm{y}}{2}}\cos\left(\frac{2\lambda_m y}{l_\mathrm{y}}\right)\cos\left(\frac{2\lambda_i y}{l_\mathrm{y}}\right)\mathrm{d}y = \begin{Bmatrix}1 & m=i\\ 0 & m\neq i\end{Bmatrix} \tag{2.59}$$

$$\frac{2}{l_\mathrm{x}}\int_{-\frac{l_\mathrm{x}}{2}}^{\frac{l_\mathrm{x}}{2}}\sin\left(\frac{2\lambda_n x}{l_\mathrm{x}}\right)\sin\left(\frac{2\pi j x}{l_\mathrm{x}}\right)\mathrm{d}x = -\frac{2\pi j(-1)^{n+j}}{\pi^2 j^2 - \lambda_n^2} \tag{2.60}$$

$$\left(\frac{\partial^2}{\partial z^2} - \left(\frac{2\lambda_m}{l_\mathrm{y}}\right)^2 - \left(\frac{2\pi j}{l_\mathrm{x}}\right)^2\right)\delta T_{jm}(z) = \sum_{n=0}^{\infty} C_{nm}\frac{v_x}{D}\frac{2\pi j(-1)^{n+j}}{\pi^2 j^2 - \lambda_n^2}\exp(-\sigma_{nm}|z|) \tag{2.61}$$

Now we assume a solution for the ordinary differential equation (2.61), $\delta T_{jm}(z) = A_{jm}\exp(-\sigma_{nm}|z|)$.

$$\frac{\partial^2}{\partial z^2}A_{jm}\exp(-\sigma_{nm}|z|) = A_{jm}\sigma_{nm}^2\mathrm{sign}(z)^2\exp(-\sigma_{nm}|z|) = A_{jm}\sigma_{nm}^2\exp(-\sigma_{nm}|z|) \tag{2.62}$$

$$\left(\sigma_{nm}^2 - \left(\frac{2\lambda_m}{l_\mathrm{y}}\right)^2 - \left(\frac{2\pi j}{l_\mathrm{x}}\right)^2\right)A_{jm} = \sum_{n=0}^{\infty} C_{nm}\frac{v_x}{D}\frac{2\pi j(-1)^{n+j}}{\pi^2 j^2 - \lambda_n^2} \tag{2.63}$$

$$\left(\left(\frac{2\lambda_n}{l_\mathrm{x}}\right)^2 - \left(\frac{2\pi j}{l_\mathrm{x}}\right)^2\right)A_{jm} = \sum_{n=0}^{\infty} C_{nm}\frac{v_x}{D}\frac{2\pi j(-1)^{n+j}}{\pi^2 j^2 - \lambda_n^2} \tag{2.64}$$

$$A_{jm} = \sum_{n=0}^{\infty} -C_{nm}l_\mathrm{x}^2\frac{v_x}{D}\frac{\pi j(-1)^{n+j}}{2(\pi^2 j^2 - \lambda_n^2)^2} \tag{2.65}$$

$$\delta T = \sum_{m,n=0}^{\infty}\sum_{j=1}^{\infty} -\frac{(-1)^{m+n+j}}{\lambda_m\sigma_{nm}}\frac{Pl_\mathrm{x}}{Ll_\mathrm{y}k}\sin\left(\frac{2\lambda_n L}{l_\mathrm{x}}\right)\frac{v_x}{D}\frac{\pi j}{\gamma_{nj}^2}\exp(-\sigma_{nm}|z|)\cos\left(\frac{2\lambda_i}{l_\mathrm{y}}y\right)\sin\left(\frac{2\pi j}{l_\mathrm{x}}x\right) \tag{2.66}$$

with $\gamma_{nj} = \pi^2 j^2 - \lambda_n^2$ a plot of this perturbation and the effect on the temperature profile can be seen in figure 2.8.

2.3.2 Wire parallel to airflow

We repeat what we did in the previous section, only now what is different is that we differentiate the temperature profile with respect to x, resulting in the following partial differential equation:

$$\nabla^2\delta T = \sum_{n,m=0}^{\infty} -C_{nm}\exp(-\sigma_{nm}|z|)\sin\left(\frac{2\lambda_m x}{l_\mathrm{x}}\right)\cos\left(\frac{2\lambda_n y}{l_\mathrm{y}}\right) \tag{2.67}$$

$$C_{nm} = \frac{2(-1)^m}{\lambda_n\sigma_{nm}}\frac{P}{Ll_\mathrm{x}^2 k}\sin\left(\frac{2\lambda_n L}{l_\mathrm{y}}\right) \tag{2.68}$$

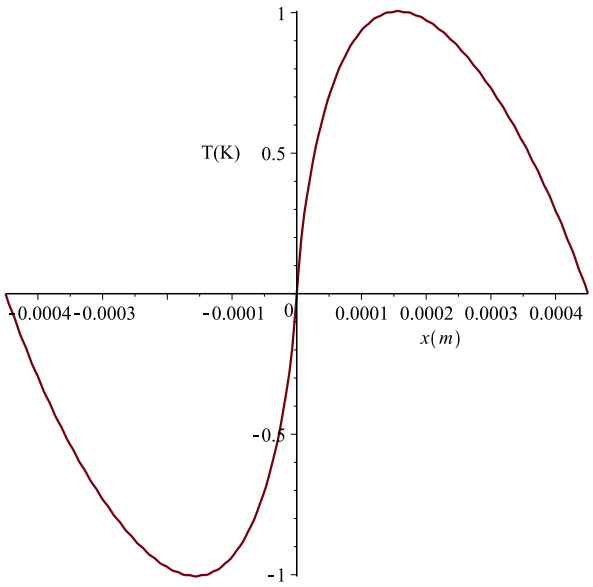

Figure 2.8: Plot of the temperature perturbation (2.72) for a flow perpendicular to the wire depending on x, with $y, z = 0$

We solve this equation using eigenfunction expansion in the same way as we did it with the airflow perpendicular to the wire. This results in an ordinary differential equation.

$$\left(\frac{\partial^2}{\partial z^2} - \left(\frac{2\lambda_n}{l_\mathrm{y}}\right)^2 - \left(\frac{2\pi j}{l_\mathrm{x}}\right)^2\right)\delta T_j(z) = \sum_{m=0}^{\infty} C_{nm}\frac{v_x}{D}\frac{2\pi j(-1)^{m+j}}{\pi^2 j^2 - \lambda_m^2}\exp(-\sigma_{nm}|z|) \tag{2.69}$$

This equation is easily solved by assuming a solution $T_j(z) = A\exp(-\sigma_{nm}|z|)$

$$\left(\sigma_{nm}^2 - \left(\frac{2\lambda_n}{l_\mathrm{y}}\right)^2 - \left(\frac{2\pi j}{l_\mathrm{x}}\right)^2\right)A = \sum_{m=0}^{\infty} C_{nm}\frac{v_x}{D}\frac{2\pi j(-1)^{m+j}}{\pi^2 j^2 - \lambda_m^2} \tag{2.70}$$

$$A = \sum_{m=0}^{\infty} -C_{nm} l_\mathrm{x}^2 \frac{v_x}{D}\frac{\pi j(-1)^{m+j}}{2(\pi^2 j^2 - \lambda_m^2)^2} \tag{2.71}$$

Combining everything the solution of the perturbation of the temperature is found:

$$\delta T = \sum_{n,m=0}^{\infty}\sum_{j=1}^{\infty} -\frac{(-1)^j}{\lambda_n \sigma_{nm}}\frac{P}{Lk}\sin\left(\frac{2\lambda_n L}{l_\mathrm{y}}\right)\frac{v_x}{D}\frac{\pi j}{\gamma_{mj}^2}\exp(-\sigma_{nm}|z|)\cos\left(\frac{2\lambda_n}{l_\mathrm{y}}y\right)\sin\left(\frac{2\pi j}{l_\mathrm{x}}x\right) \tag{2.72}$$

with $\gamma_{mj} = \pi^2 j^2 - \lambda_m^2$ a plot of this perturbation affecting the temperature profile can be seen in figure 2.9

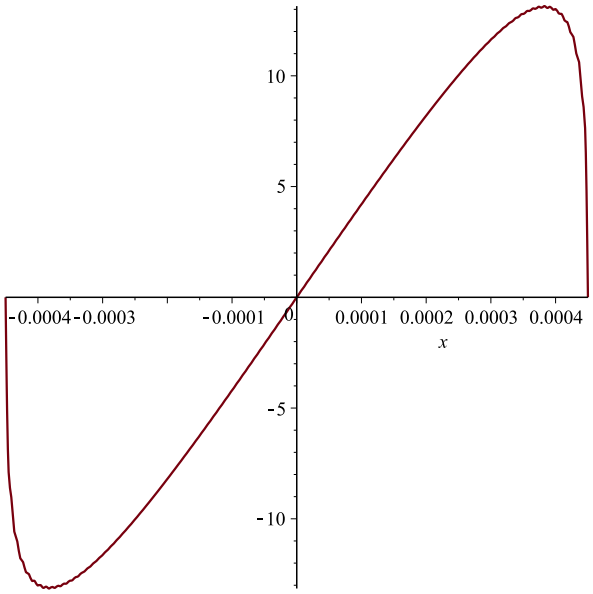

Figure 2.9: Plot of the temperature perturbation (2.66) due to a flow parallel to the wire depending on x, with $y, z = 0$

2.4 Dynamic disturbance thermal profile

2.4.1 Flow perpendicular to the wire

Using the same heat equation as in the previous section, with the same assumptions,

$$\rho c_p \left(\frac{\partial}{\partial t} T + \mathbf{v} \nabla T \right) - \nabla (k \nabla T) = Q \tag{2.73}$$

but now we don't assume the time dependence to be zero. The sensor deals with sound waves, which are acoustic, so we assume the incoming particle velocity to be $v = v_0 \exp(i2\pi f t)$. Due to this being the only time depending term in the heat equation, we can also assume the solution to be of the form $\delta T(x, y, z, t) = \delta T(x, y, z) \exp(i2\pi f t)$. Using that we only have an x component of the particle velocity $\mathbf{v} = (v, 0, 0)$ we get for the convective term $\mathbf{v} \nabla T = v \frac{\partial}{\partial x} T$.

$$\frac{i2\pi f}{D} \delta T - \nabla^2 \delta T = -\frac{v_0}{D} \frac{\partial}{\partial x} T \tag{2.74}$$

This is almost the same equation as we had in the previous section and we can solve it in the same way using eigenfunction expansion. First we begin with constructing a solution for the perturbation of the temperature for the wire perpendicular to the x direction.

$$\left(-\frac{i2\pi f}{D} + \frac{\partial^2}{\partial z^2} - \left(\frac{2\lambda_m}{l_y} \right)^2 - \left(\frac{2\pi j}{l_x} \right)^2 \right) \delta T_{jm}(z) = \sum_{n=0}^{\infty} C_{nm} \frac{v_0}{D} \frac{2\pi j (-1)^{n+j}}{\pi^2 j^2 - \lambda_n^2} \exp(-\sigma_{nm} |z|) \tag{2.75}$$

$$C_{nm} = \frac{2(-1)^m}{\lambda_m \sigma_{nm}} \frac{P}{L l_y l_x k} \sin\left(\frac{2\lambda_n L}{l_x} \right) \tag{2.76}$$

$$\tag{2.77}$$

The above equation can be solved by assuming $\delta T_{jm}(z) = A_{jm}\exp(-\sigma_{nm}|z|)$.

$$A_{jm} = \sum_{n=0}^{\infty} C_{nm}\frac{v_0}{D}\frac{2\pi j(-1)^{n+j}}{\left(\pi^2 j^2 - \lambda_n^2\right)K_{nj}} \tag{2.78}$$

$$K_{nj} = \left(\frac{2\lambda_n}{l_\mathrm{x}}\right)^2 - \left(\frac{2\pi j}{l_\mathrm{x}}\right)^2 - \frac{i2\pi f}{D} \tag{2.79}$$

Putting everything back together gives the temperature perturbation for a flow perpendicular to the wire.

$$\begin{aligned}\delta T(x,y,z,t) = \sum_{n,m=0}^{\infty}\sum_{j=1}^{\infty}\frac{2(-1)^m}{\lambda_m\sigma_{nm}}\frac{P}{Ll_\mathrm{y}l_\mathrm{x}k}\sin\left(\frac{2\lambda_n L}{l_\mathrm{x}}\right)\frac{v_0}{D}\frac{2\pi j(-1)^{n+j}}{\left(\pi^2 j^2-\lambda_n^2\right)K_{nj}} \\ \times\cos\left(\frac{2\lambda_m}{l_\mathrm{y}}y\right)\sin\left(\frac{2\pi j}{l_\mathrm{x}}x\right)\exp(-\sigma_{nm}|z|)\exp(i2\pi f t)\end{aligned} \tag{2.80}$$

2.4.2 Flow parallel to the wire

For the flow parallel to the wire we can do the same as we did above only now we have a different $\frac{\partial}{\partial x}T$ term. After eigenfunction expansion that leads to the following equation.

$$\left(-\frac{i2\pi f}{D}+\frac{\partial^2}{\partial z^2}-\left(\frac{2\lambda_n}{l_\mathrm{y}}\right)^2-\left(\frac{2\pi j}{l_\mathrm{x}}\right)^2\right)\delta T_{jn}(z) = \sum_{m=0}^{\infty}C_{nm}\frac{v_0}{D}\frac{2\pi j(-1)^{m+j}}{\pi^2 j^2-\lambda_m^2}\exp(-\sigma_{nm}|z|) \tag{2.81}$$

$$C_{nm} = \frac{2(-1)^m}{\lambda_n\sigma_{nm}}\frac{P}{Ll_\mathrm{x}^2 k}\sin\left(\frac{2\lambda_n L}{l_\mathrm{y}}\right) \tag{2.82}$$

Using that $\delta T_{jn} = A_{jn}\exp(-\sigma_{nm}|z|)$ results in the following equation.

$$A_{jn} = \sum_{m=0}^{\infty}C_{nm}\frac{v_0}{D}\frac{2\pi j(-1)^{m+j}}{\left(\pi^2 j^2-\lambda_m^2\right)K_{mj}} \tag{2.83}$$

$$K_{mj} = \left(\frac{2\lambda_m}{l_\mathrm{x}}\right)^2 - \left(\frac{2\pi j}{l_\mathrm{x}}\right)^2 - \frac{i2\pi f}{D} \tag{2.84}$$

Combining everything results in the temperature perturbation for the flow parallel to the wire.

$$\begin{aligned}\delta T(x,y,z,t) = \sum_{n,m=0}^{\infty}\sum_{j=1}^{\infty}\frac{2}{\lambda_n\sigma_{nm}}\frac{P}{Ll_\mathrm{x}^2 k}\sin\left(\frac{2\lambda_n L}{l_\mathrm{y}}\right)\frac{v_0}{D}\frac{2\pi j(-1)^j}{\left(\pi^2 j^2-\lambda_m^2\right)K_{mj}} \\ \times\cos\left(\frac{2\lambda_n}{l_\mathrm{y}}y\right)\sin\left(\frac{2\pi j}{l_\mathrm{x}}x\right)\exp(-\sigma_{nm}|z|)\exp(i2\pi f t)\end{aligned} \tag{2.85}$$

2.5 Sensitivity

To calculate the sensitivity we first calculate the average temperature of the perturbation over the wires. To calculate this average, integration over the temperature perturbation is performed over the length, width and thickness of the upper part of the wire.

$$\frac{1}{2L}\int_{-L}^{L}\cos\left(\frac{2\lambda_m y}{l_\mathrm{y}}\right)\mathrm{d}y = \frac{l_\mathrm{y}\sin\left(\frac{2\lambda_m y}{l_\mathrm{y}}\right)}{2L\lambda_m} \tag{2.86}$$

$$\frac{2}{l_\mathrm{x}}\int_0^{\frac{l_\mathrm{x}}{2}}\sin\left(\frac{2\pi j x}{l_\mathrm{x}}\right)\mathrm{d}x = -\frac{((-1)^j-1)}{\pi j} \tag{2.87}$$

$$\exp(-\sigma_{nm}|z|)\delta(z) = 1 \tag{2.88}$$

Contribution from wire parallel to flow

$$\Delta T = \sum_{n,m=0}^{\infty}\sum_{j=1}^{\infty} -\frac{2}{\lambda_n \sigma_{nm}}\frac{P}{L l_x^2 k}\sin\left(\frac{2\lambda_n L}{l_y}\right)\frac{v_0}{D}\frac{2\pi j(-1)^j}{\left(\pi^2 j^2 - \lambda_m^2\right)K_{mj}} \tag{2.89}$$

$$\times \frac{l_y \sin\left(\frac{2\lambda_n L}{l_y}\right)}{2L\lambda_n}\frac{((-1)^j - 1)}{\pi j}\exp(i2\pi f t)$$

Contribution from wire perpendicular to flow

$$\Delta T = \sum_{n,m=0}^{\infty}\sum_{j=1}^{\infty} -\frac{2(-1)^m}{\lambda_m \sigma_{nm}}\frac{P}{L l_y l_x k}\sin\left(\frac{2\lambda_n L}{l_x}\right)\frac{v_0}{D}\frac{2\pi j(-1)^{n+j}}{\left(\pi^2 j^2 - \lambda_n^2\right)K_{nj}} \tag{2.90}$$

$$\times \frac{l_y \sin\left(\frac{2\lambda_m L}{l_y}\right)}{2L\lambda_m}\frac{((-1)^j - 1)}{\pi j}\exp(i2\pi f t) \tag{2.91}$$

From this averaged temperature we can calculate the resistance

$$R = R_0(1 + \alpha\Delta T) \tag{2.92}$$

In [3] values for $R_0 = 683\,\Omega$ and $\alpha = 8.6 \times 10^{-4}\,\mathrm{K}$ were derived.
From the resistance we can calculate the voltage difference between the two terminals. The temperature difference of the upper and lower part of the wire are opposite which means that the resistance is also opposite.

$$V_{2+} - V_{2-} = I(R_1 - R_2) = 2IR_0\alpha\Delta T \tag{2.93}$$

2.5.1 Comparison with measurements

A comparison between the experimental and theoretical frequency characteristics is shown in figure 2.10. The analytical model is plotted using the particle velocities measured in the sound source which were measured simultaneously with the voltage of the sensor. Therefore there is noise in the model curve were you normally wouldn't expect that. The two curves look somewhat similar, but it looks like there is at least one element missing. This element could be the simplification that the heat capacity and density of the wires do not play a role in the temperature perturbation. The effect of this simplification is hard to predict, in previous studies [3] the heat capacity and density of the wires only resulted in a second tipping point where after the sensitivity dropped more, this tipping point is around 1300 Hz. But due to a different sensing method, measuring mostly in the longitudinal direction the heat capacity and density will have a bigger impact.

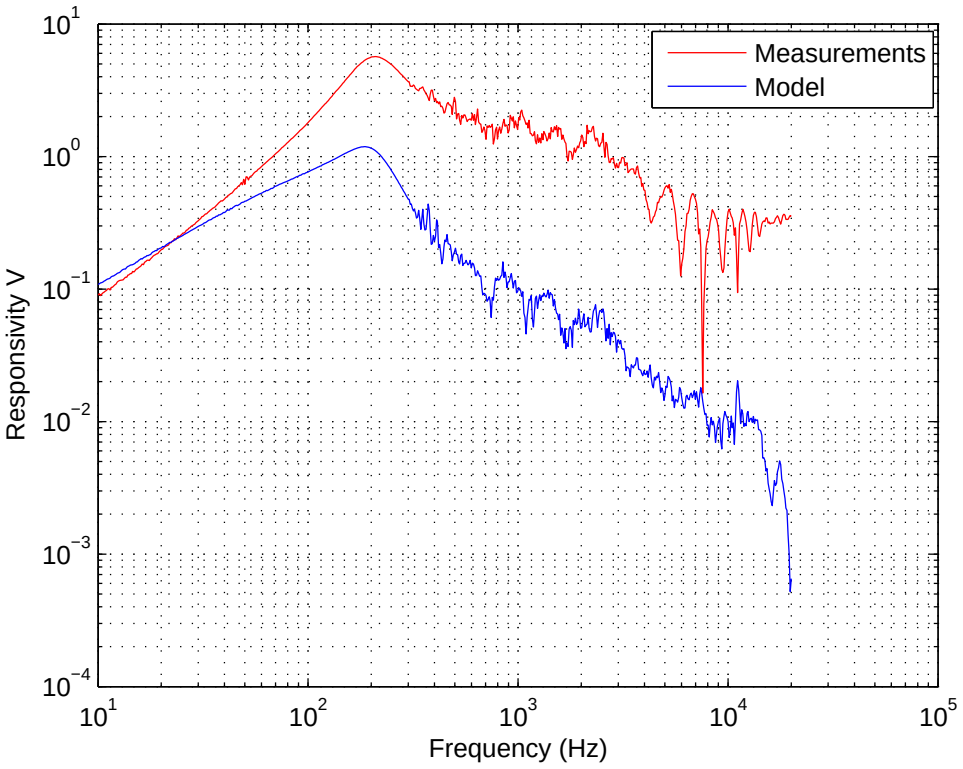

Figure 2.10: The voltage measured from the crossed wire sensor and calculated with the analytical model, for a flow with certain frequencies

Chapter 3

Reduced model

In this chapter I will be looking at the possibility of reducing (decreasing the sums in an equation to an equation that consists of only a few terms) the equation for the thermal profile and it's perturbations.

3.1 Thermal profile

The equation for the thermal profile is as follows

$$T(x,y,z) = \sum_{n=0}^{\infty}\sum_{m=0}^{\infty} \frac{(-1)^m}{\lambda_m \lambda_n \sigma_{nm}} \frac{P}{L l_y k} \sin\left(\frac{2\lambda_n L}{l_x}\right) \exp(-\sigma_{nm}|z|) \cos\left(\frac{2\lambda_m y}{l_y}\right) \cos\left(\frac{2\lambda_n x}{l_x}\right) \tag{3.1}$$

$$\sigma_{nm} = \sqrt{\left(\frac{2\lambda_n}{l_x}\right)^2 + \left(\frac{2\lambda_m}{l_y}\right)^2} \tag{3.2}$$

$$\lambda_m = \frac{\pi}{2}(2n+1) \tag{3.3}$$

To determine if the equation could be reduced, plots were made in the following way. The sum-variable that was investigated was substituted with zero while the other sum-variable(s) were summed to a hundred, this was plotted, and then it was substituted for one, etc. up to one hundred. This resulted in the following graphs figure 3.1 and 3.2. From these graphs you can easily see that you only need a few terms of m to have a quite a good approximation, for n this isn't the case and you will need to go up to quite a large number.

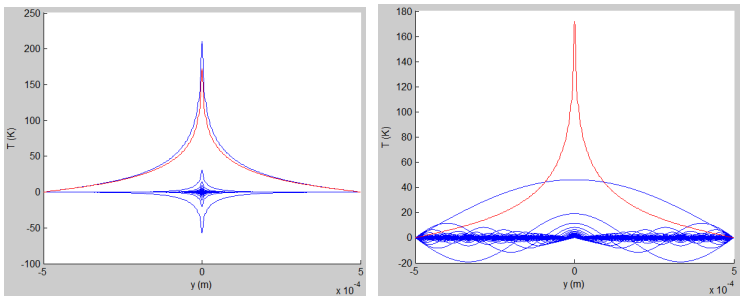

(a) m (b) n

Figure 3.1: Plots of how the values of m and n (blue) contribute to the thermal profile (red). For the wire perpendicular to the y-axis

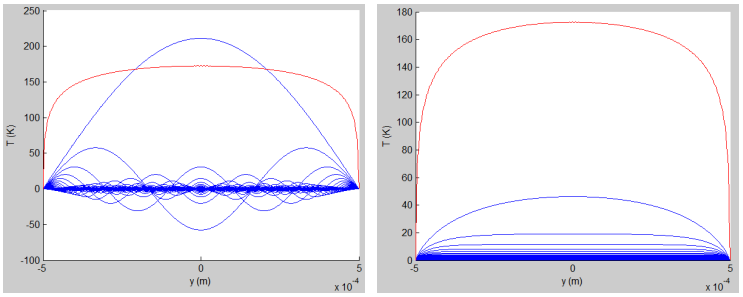

(a) m (b) n

Figure 3.2: Plots of how the values of m and n (blue) contribute to the thermal profile (red). For the wire parallel to the y-axis

3.2 Perturbation flow parallel

The equation for the temperature perturbation with a flow parallel to the wire, with $\gamma_{nj} = \pi^2 j^2 - \lambda_n^2$

$$\delta T(x,y,z,t) = \sum_{n,m=0}^{\infty} \sum_{j=1}^{\infty} \frac{2}{\lambda_n \sigma_{nm}} \frac{P}{L l_x^2 k} \sin\left(\frac{2\lambda_n L}{l_y}\right) \frac{v_0}{D} \frac{2\pi j(-1)^j}{\left(\pi^2 j^2 - \lambda_m^2\right) K_{mj}} \times \cos\left(\frac{2\lambda_n}{l_y} y\right) \sin\left(\frac{2\pi j}{l_x} x\right) \exp(-\sigma_{nm}|z|) \exp(i2\pi f t) \tag{3.4}$$

Plotting this equation in the same way we did as in the previous section we get the following graphs, figure 3.3. As can be seen, for m and j you need to sum to at least 3-5 terms. For n this is a lot more, in the range of 50-100 terms.

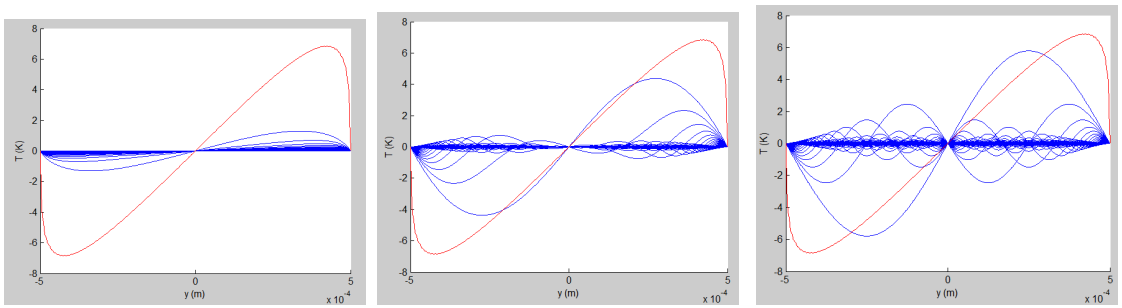

(a) n (b) m (c) j

Figure 3.3: Plots of how the values of m and n (blue) contribute to the total plot (red). For the wire parallel to the y-axis and also the flow parallel to the y-axis

3.3 Perturbation flow perpendicular

The equation for the temperature perturbation with a flow perpendicular to the wire

$$\delta T(x,y,z,t) = \sum_{n,m=0}^{\infty}\sum_{j=1}^{\infty} \frac{2(-1)^m}{\lambda_m \sigma_{nm}} \frac{P}{L l_y l_x k} \sin\left(\frac{2\lambda_n L}{l_x}\right) \frac{v_0}{D} \frac{2\pi j(-1)^{n+j}}{\left(\pi^2 j^2 - \lambda_n^2\right) K_{nj}} \times \cos\left(\frac{2\lambda_m}{l_y} y\right) \sin\left(\frac{2\pi j}{l_x} x\right) \exp(-\sigma_{nm}|z|) \exp(i2\pi f t) \tag{3.5}$$

Plotting this equation in the same way as in the previous sections results in figure 3.4, m and j only need a few 1-3 terms to describe the perturbation, but for n some more terms 10-15 are needed.

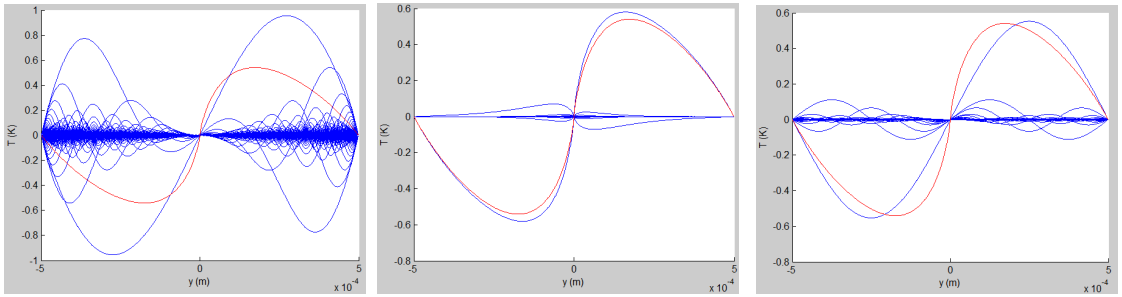

(a) n (b) m (c) j

Figure 3.4: Plots of how the values of m and n (blue) contribute to the total plot (red). For the wire perpendicular to the y-axis and the flow parallel to the y-axis

Chapter 4

Exploration parameter space

In this chapter I will explore how the different parameters of the micro-flown affect the sensitivity, the averaged temperature of the perturbation, over a frequency range.

4.1 Square chip $l_y = l_x$

In this section we will look at how the length of the wires affects the temperature of the perturbation, with $l_y = l_x$ such that the sensor will have the same sensitivity in both directions. From figure 4.1 you can see that a smaller length of the wires results in a higher corner frequency, but the sensitivity before this corner frequency will be somewhat smaller.

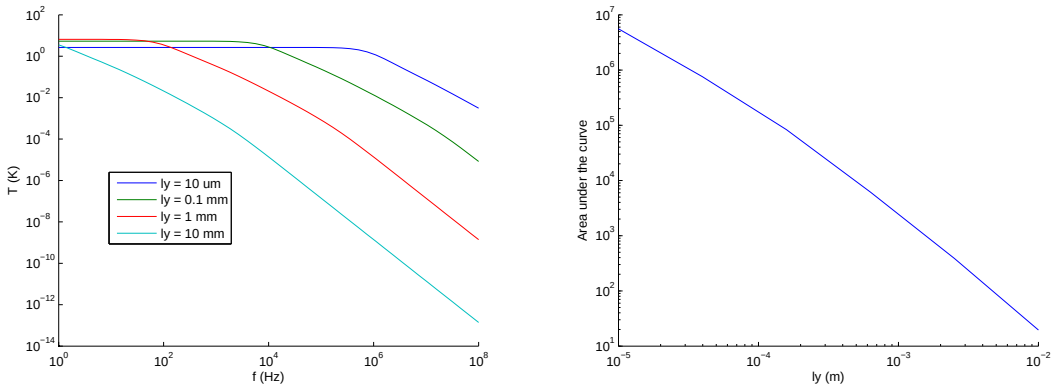

(a) (b)

Figure 4.1: (a) The averaged temperature plotted as a function of frequency for various values of l_y (b) The area under the curve of (a) plotted against l_y

4.2 Width of the wire

Now we will look how the average temperature of the perturbation changes as we change the width (L) of the wire. As can be seen in figure 4.2 it looks like the sensitivity only changes when the value of L approaches that of $l_y = 1 \times 10^{-3}$ m.

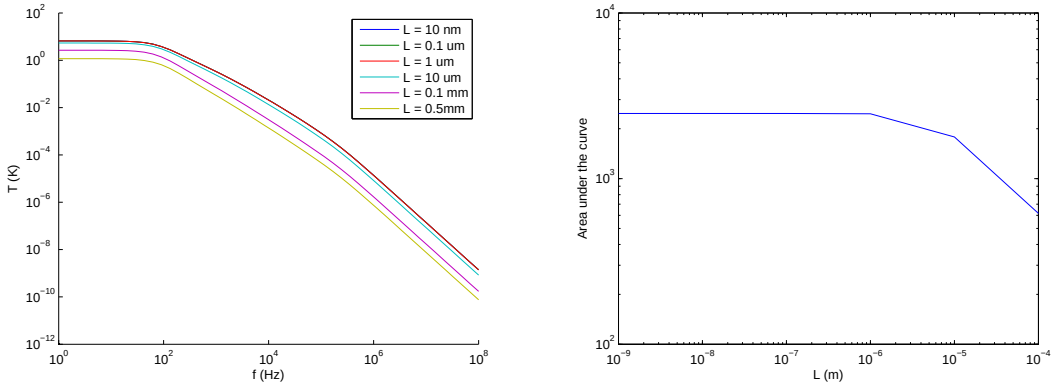

(a) (b)

Figure 4.2: (a) The averaged temperature plotted as a function of frequency for various values of L (b) The area under the curve of (a) plotted against L.

Chapter 5

Discussion and Conclusion

5.1 Discussion

In the development of the analytical model a few simplifications and assumptions were made. The air thermal conductivity (k) was considered independent of temperature, in the temperature range the sensor operates 500 °C, k doubles, so that assumption isn't really valid. We didn't take into account the bottom of the sensor at a negative z and we assumed the walls to be extending from the positive z. But as can be seen in figure 2.7 a simulation with the accurate geometry of the sensor has almost the same temperature profile. Unfortunately due to time constrains we were not able to measure the actual thermal profile of the sensor to compare it to the model.
The sensitivity according to the analytical model has roughly the same shape compared to the measurements of the sensitivity, but the analytical model shows a stronger decay with frequency than observed in the measurements. This could either be due to

- one of the assumptions made or due to incomplete incorporation of all effects, e.g. such as the heat capacity and thermal conductivity of the wires
- from a mistake in the derivation of the dynamic disturbance
- or because the wires have a thicker connection with the walls of the sensor, which leads effectively to a smaller wire.

These are subjects that could be examined in future work in order to further improve the model.

5.2 Recommendations

- Look more into noise
- Make a series of crossed wire flowns with varying length to validate influence of length on performance
- Validate the thermal profile by measurements
- Expand the analytical model to include the heat capacity and density of the wires

5.3 Conclusion

In this report an analytical model for the crossed-wire particle velocity sensor has been constructed. This started with an expression for the thermal profile (2.47). This expression was subsequently used in the construction of expressions for the static flow disturbances of the temperature for the separate direction of the wire (2.66) (2.72) and for the the construction of the dynamic disturbance of the temperature (2.80) (2.85). Unfortunately these equations can not be simplified to reduced equations, implying that summations of functions will still be needed to describe thermal fields with sufficient accuracy. A conclusion that can be made from the exploration of the parameters is that a reduction in both width and length increases the frequency range of the sensor, however, without significantly reducing the sensitivity of the sensors. This conclusion does indicate some potential for future large bandwidth sensors, albeit that the simplifications made to allow for the model to be made need to be carefully checked against experimental results. Moreover, not only the effects of the geometry on the sensitivity but also the corresponding implications for the thermal (Johnson-Nyquist) noise need to be investigated.

Bibliography

[1] Richard Haberman. *Elementary applied partial differential equations*. Prentice Hall Englewood Cliffs, NJ, 1983.

[2] O Pjetri, RJ Wiegerink, TSJ Lammerink, and GJM Krijnen. A crossed-wire 2-dimensional acoustic particle velocity sensor. In *Sensors, 2013 IEEE*, pages 1–4. IEEE, 2013.

[3] VB Svetovoy and IA Winter. Model of the μ-flown microphone. *Sensors and Actuators A: Physical*, 86(3):171–181, 2000.

[4] JW van Honschoten, GJM Krijnen, VB Svetovoy, HE de Bree, and MC Elwenspoek. Analytic model of a two-wire thermal sensor for flow and sound measurements. *Journal of Micromechanics and Microengineering*, 14(11):1468, 2004.